Synthesis, Characterization, Computational Studies, and Evaluation of Neuroprotective Effects of New Piperazine Compounds

Erfantalab, Malihe
University of Applied Science and Technology, Arak, I.R. IRAN

Eskandari, Najmeh; Momeni, Hamid Reza*[+]
Department of Biology, Arak University, Arak, I.R. IRAN

Khanmohammadi, Hamid
Department of Chemistry, Arak University, Arak, I.R. IRAN

ABSTRACT: *The new piperazine-based Schiff base hydrazone with N, O donor set of atoms,* ***LPE****, has been prepared by the condensation reaction of new piperazine-based diamine,* ***APE****, with salicylaldehyde. The structure of newly prepared compounds was characterized by using FT-IR, UV-Vis,* ^{1}H *NMR, and* $^{13}C\{^{1}H\}$*-spectroscopic methods as well as elemental analysis data. Furthermore, the structure of piperazine-based compounds,* ***APE*** *and* ***LPE****, has been optimized and the geometrical structures of a diamine compound,* ***APE****, and Calcium atom have been investigated at the level of density functional theory (DFT). The 6-311++G(d,p) basis set was utilized for ligands in the gas phase. The optimized structures contain N…Ca interactions and piperazine rings have boat structure in most of them. The chelating structures of piperazine rings show most stabilization among other interactions, the stabilization energy is -1493.9667 kJ* mol^{-1}*. Also, the prepared compounds were evaluated for preventive effect on apoptotic motor neurons in adult mouse spinal cord slices. The* ***APE*** *inhibited apoptosis in the motor neurons and significantly increased viability in these neurons.*

KEYWORDS: *Piperazine; Schiff base; Hydrazone; Neuroprotective effects; DFT calculation.*

INTRODUCTION

Recent years have seen much-heightened interest in the synthesis, structural characterization, and physical property measurements of piperazine compounds, because of these special chemicals, physical and biological properties [1-4]. Piperazine compounds represent an important class of organic molecules because of their flexible structure. The four distinct conformations can be devoted to piperazine moiety: chair, boat, twist-boat, and half-boat, which the former is the most favorable thermodynamically [5]. The piperazine unit, in the boat and twist-boat forms, chelates one or bridges two metal ions while in the chair conformation, each nitrogen can bridge pair metals [5-7].

* *To whom correspondence should be addressed.*
+ E-mail: h-momeni@araku.ac.ir
1021-9986/2021/2/477-486 10/$/6.00

This special behavior can cause piperazine to show special structures with various properties such as molecular switch [8], molecular magnetism [9], anthelmintic [10], antimicrobial [11-12], acetylcholinesterase inhibition [13], melanocortin-4-receptor (MC4-R) [14], drug designer [15], anti-PAF [16], anti-HIV [17] and anti-obesity [18] activities.

Recently, piperazine-based ligands have also attracted increasing attention due to their interesting chiral/achiral and geometrical features in connection with their application for molecular memory storages [19], nonlinear optical elements [20] and biological–medical studies [21,10]. Therefore, several studies have been published on the synthesis and spectral properties of piperazine-based hydrzone compounds, as well as their transition metal complexes [22–25]. Among the plethora of new synthetic piperazine- based ligands those containing N, O and S donor atoms are of particular interest for several reasons. Compounds with more donating atoms are noteworthy compounds with rich and well-known chemistry [26–28]. The incorporation of various donating atom type into acyclic and/or macroacyclic ligands has facilitated the isolation of a wide range of transition metal complexes with interesting biological and magnetic properties [29–31]. Also, their chelating properties make them suitable for analytical studies [32,33].

On the other hand, symmetrical N donor compounds have been found a key pharmacological element or an important structural cradle in a large number of drugs that include a wide range of biochemical goals [34,35]. Among them, symmetrical piperazine-based hydrazones with more donor atoms are used as a building block in drug synthesis and macromolecular building blocks because piperazine moiety is a good hydrogen-bond acceptor, which can adopt various conformations or acts as chelating agent [36]. Some representative examples include photochromic properties [37], analytical applications [32] and also acting as neuroprotective substances in a variety of neurons such as mesencephalic [38], cerebral [39] and substantia nigra [40] neurons.

Based on an abiding interest in designing Schiff base ligands, especially with various donor atoms, for selectively discriminating metal ions, and incorporating distinctively pharmacological moieties, we report here the newly prepared piperazine-based compounds (Fig. 1). The compounds have been characterized by spectroscopic methods (^{1}H NMR, UV–Vis and IR) as well as elemental analysis data. We hypothesized that the prepared compounds might display neuroprotective effect and delay apoptosis in motor neurons. To test this hypothesis, we used adult mouse spinal cord slices to examine the effect of piperazine-based compounds on the apoptosis of motor neurons in cultured slices. Fluorescent staining was used to determine apoptotic cell death based on morphological changes. Surprisingly, the 1,2-bis(4-(2-aminoethyl)piperazine)ethane, APE, shows neuron protective effect. Also, the structure of new piperazine-based compounds have been optimized with the B3LYP functional; and the interaction of calcium and APE (in 1:1 ratio), based on neuroprotection effects, have been studied at the level of Density Functional Theory (DFT) using 6-311++G(d,p) basis set.

EXPERIMENTAL AND THEORETICAL SECTION

Materials

All of involved reagents and solvents were of analytically grade and used as received without further purification. Salicylaldehyde, 2-aminoethylpiperazine, phthalic anhydride and dibromoethane were obtained from Aldrich and Merck.

Instrumentation

The structure of all synthesized compounds was confirmed by ^{1}H NMR and ^{13}C{^{1}H] spectra, recorded on a Bruker AV 300 MHz spectrometer. FT-IR spectra were recorded as pressed KBr discs, using Unicom Galaxy Series FT-IR 5000 spectrophotometer in the region of 400-4000 cm^{-1}. Melting points were determined on Electrothermal 9200 apparatus. C.H.N. analysis were performed on a Vario EL III elemental analyzer. Electronic spectral measurements were carried out using Agilent hp 8453 spectrophotometer in the range 300-800 nm using 1 cm path quartz cells. The measurements were performed at 25 (±0.5) °C.

Theoretical calculations

The structure data in gas phase were calculated using Gaussian-03 [41] series of programs. A starting molecular mechanics structure for the DFT calculations was obtained using the HyperChem 5.02 program (Hypercube, Inc. Gainesville). The geometry of the prepared compound was fully optimized at the B3LYP/6-311++G(d,p) level. Vibrational frequency analysis, calculated at the 6-31+G* level of theory, indicate that the optimized structure is

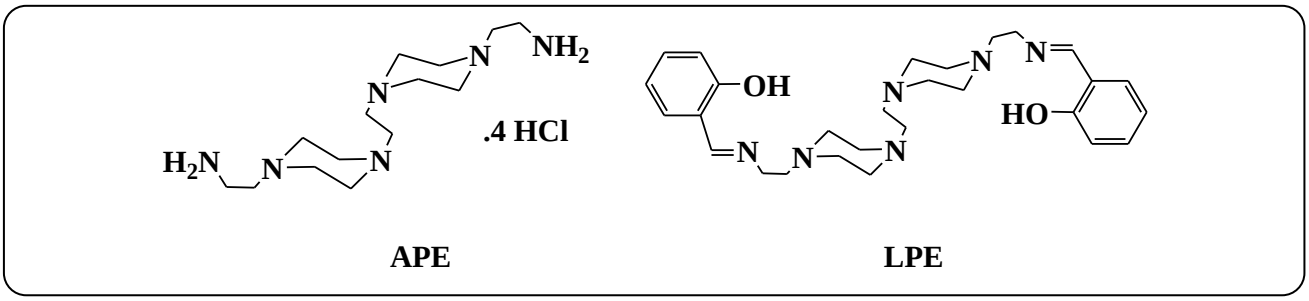

Fig. 1: The synthesized piperazine-based compounds.

at the stationary points corresponding to global minima without any imaginary frequency.

Animals and the culture of spinal cord slices

Adult female NMRI mice (23-25 gr) were purchased from Pasture Institute, Tehran, Iran. The animals were housed in plastic cages at 20°C, a 12-Hours light/ dark cycle with water and food *ad libitum*. The experiments were approved by the local ethical committee at Arak University. The animals were deeply anesthetized by intraperitoneal injection of sodium pentobarbital (60 mg/kg) and subsequently killed by heart puncture. The spinal cord was dissected and placed in ice-cold phosphate-buffered saline (PBS, pH 7.4). The thoracic region of the spinal cord [42] was then sliced transversally into 500 µm-thick sections using a McIlwain tissue chopper (Stoelting, USA). The slices were cultured in a medium (50% minimum essential medium, 25% Hanks balanced salt solution, 25% horse serum, 25 mM HEPES, 6g/L glucose and penicillin-streptomycin, pH 7.3-7.4) in the absence (control) or presence of piperazine derivatives. The cultured slices were then incubated at 37°C in a humidified atmosphere of 5% CO_2 in air for 24 hours.

Fixation and sectioning

Freshly prepared (0 hour) and cultured slices were fixed in Stefanini's fixative (2% paraformaldehyde, 0.2% picric acid in 0.1 M phosphate buffer, pH 7.2) for at least 2 hours. The fixed slices were washed in PBS (3×5 min) and incubated overnight in 20% sucrose in PBS at 4°C. The slices were cut into 10 µm-thick sections in a cryostat. The sections were collected and mounted on Poly-L-lysine coated glass slides.

Assessment of apoptosis

To study morphological features of apoptosis, a combination of propidium iodide (Sigma, USA, 10 µg/mL in PBS, 15 min at room temperature) and Hoechst 33342 (Sigma, USA, 5 µg/ml in PBS, 1 min at room temperature) was used. The cryostat sections were washed in PBS (3×5 min) and mounted in glycerol/PBS (1:1) and coverslipped. Photographs were taken with an Olympus camera attached to an Olympus fluorescence microscope (Olympus Optical Co Ltd, Japan) using the appropriate excitation and emission filters.

Chemicals

All the synthesized materials were dissolved in PBS as stock solutions. Each solution was directly added to the medium and tested with 25, 50, 100, and 200 µM to find the effective concentration. The controls received a corresponding amount of PBS.

Statistical analysis

Results were expressed as mean ±SD. The statistical significances were analyzed by analysis of variance (ANOVA). In all cases, tests were considered significant at the level of $p<0.05$.

Synthesis

Synthesis of 1,2-bis(4-(2-aminoethyl)piperazine)ethane, APE

The diamine compound was prepared according to the literature method [43]. 2-Aminoethylpiperazine (2.58 g, 20 mmol) and phthalic anhydride (2.96 g, 20 mmol) were mixed in appropriate beaker and fused at 180 °C with constant stirring for 15 min. After lowering the temperature (at about 160 ° C), dibromoethane (1.88 g, 10 mmol) was also added and fused together with constant stirring for 30 min. The resulting solid was washed in two steps with hot ethanol, pulverized and heated under reflux with HCl (300 ml, 25%) for 12 h. The phthalic acid which was formed on cooling was filtered off and the filtrate

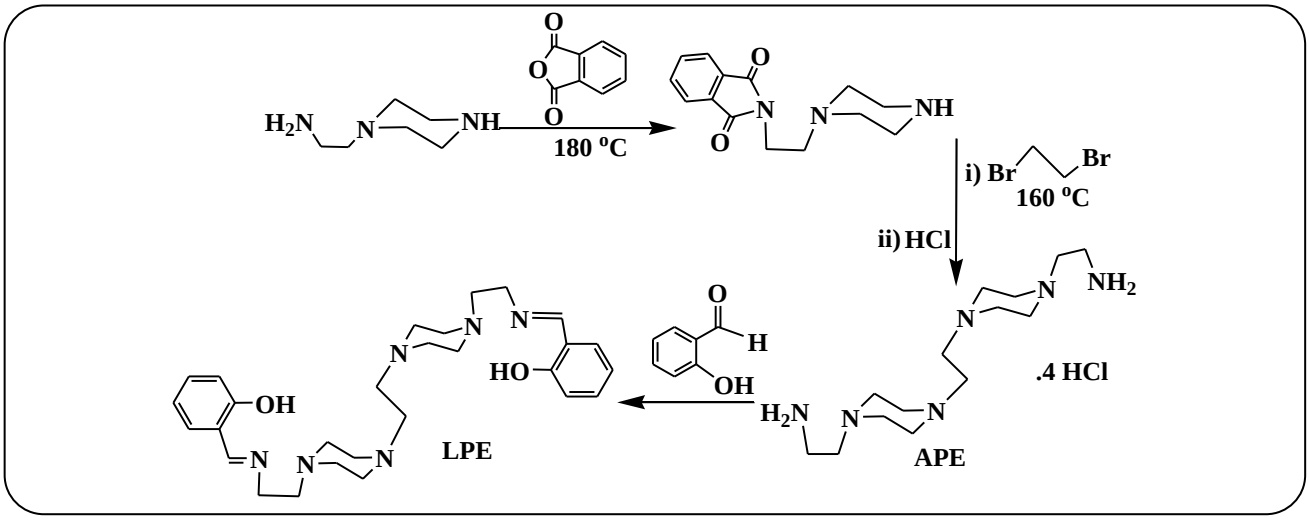

Scheme 1: The processes of synthesis of 1,2-bis(4-(2-aminoethyl)piperazine)ethane, APE, and1, 2-bis(4-(2-((E)- (imino)methyl)phenol)piperazine)ethane LPE

was evaporated to small bulk and poured into absolute ethanol. The resulting viscous precipitate was recrystallized from EtOH/H_2O, washed with a small amount of cooled absolute ethanol and diethyl ether, and the resulting yellow powder was dried (see supporting information); and characterized as the pure compound (Scheme 1). Yield: 2.15 g (31%), m.p:>300 ºC. IR (KBr, cm^{-1}); 3464(N-H stretch), 1631, 1471, 1438, 1396, 1356, 1003, 927, 885, 717, 530. ^{1}H NMR δ_H (DMSO -d_6, ppm): 3.79 (t, CH_2, 4H), 2.66 (bs, piperazine and CH_2, 10H).Anal. Calc. for $C_{14}H_{38}Cl_4N_6O$: C, 37.56; H, 8.49; N, 18.75. Found: C, 37.6; H**,** 8.4**;** N, 18.7%.

Synthesis of 1,2-bis(4-(2-((E)- (imino)methyl)phenol) piperazine)ethane, LPE

A solution of KOH (0.112 g, 2 mmol) in absolute ethanol (10 mL) was added to a suspension of the appropriate APE salt (0.166 g, 0.5 mmol) in absolute ethanol (10 mL). The mixture was stirred at room temperature for a few minutes then filtered, and the precipitate was washed well with absolute ethanol (0.122 g, 10 mL). The washings and the filtrate were combined and this solution was added to a hot solution of salicylaldehyde (1 mmol) in absolute methanol (20 ml). After refluxing, the solution was filtered for 24 h The precipitate was filtered and washed with hot ethanol three times (Scheme 1). The resulted product was dried in air (*see supporting information*).Yield: 67.8 %, m.p 162 ºC. IR (KBr, cm^{-1}); 1635 υ(C=N), 1610(C=C), 1579, 1498, 1462, 1305, 1282, 1161, 1136, 1006, 895, 858, 754, 738. UV-Vis λmax(nm)(ε ($M^{-1}cm^{-1}$)) in DMSO: 260(52667), 315(14167). ^{1}H NMR δ_H (DMSO -d_6, ppm): 13.64(s,br,OH, 2H), 8.55(s, imine, 2H,), 7.42(dd, phenyl, 2H, J1= 1/40 Hz, J2= 7/60 Hz), 7.32 (dt, phenyl, 2H, J1= 1/60 Hz, J2= 7/80 Hz), 6.87(m, phenyl, 4H), 3.69(t, CH_2, 4H), 2.57 (t, CH_2,4H), 2.51(m, piperazine, 16H), 2.36 (s, CH_2,4H). ^{13}C {^{1}H} δ_C (DMSO-d_6, ppm): 52.835, 53.146, 55.414, 58.084, 116.551, 118.272, 118.568, 131.523, 132.215, 160.965, 166.304. Anal. Calc. for $C_{28}H_{42}N_6O_3$: C, 65.85; H, 8.29; N, 16.46 %. Found: C, 67.1; H, 8.0; N, 16.3 %.

RESULT AND DISCUSSION

Characterization

The IR spectrum of LPE contains stretching bands at 1635 cm^{-1} which are assigned for azomethine, C=N band [44-45]. The ^{1}H NMR spectrum of the LPE contains slightly broad signals in the region 13.64 ppm assigned to OH protons, as were confirmed by deuterium exchange when D_2O was added to d_6-DMSO solution. The CH=N imine protons exhibit a singlet resonance in 8.55 ppm. Electronic absorption spectra of the LPE recorded in DMSO, display mainly two bands. The first band located around 260-295 nm may be assigned for to π-π* aromatic rings transitions [46]. The weak broad absorption band at 310–355nm may be assigned to the n– π* and π-π* electronic transition associated with the C=N. In the IR spectrum of APE three bands at 3464, 1396 and 717 cm^{-1} can be attributed to N-H stretch, C-N stretch and N-H wag.

Respectively. The ^{1}H NMR spectrum of the APE contains broad signals in 2.66 ppm are assigned to piperazine and ethyl protons. One slight broad triplet signal at 3.79 ppm can be assigned to CH_2 protons.

Computational results: Interaction energy and geometry

The APE and calcium atom interactions have been investigated using optimized structure of the most stable configurations of corresponding APE compound *(see supporting information)*. All the found minima have been gathered in Fig. 2 with some of the intermolecular distances.

Association of a calcium atom with APE gives two 1:1 interactions which are denoted as CaAPE1 and CaAPE2 (Fig. 1). In CaAPE1 complex, one of the NH_2 moieties points toward the position of the Calcium atom. The calculated distance between the interacting atoms is 2.568 A°. The stabilization energy obtained for this structure is only -1482.4321 kJ/mol. In the CaAPE2 binary complex, one of the N moieties of piperazine ring interacts with Calcium atom. The N-Ca interacting found 2.619 A°, and the stabilization energy of the complex is -1481.0711 kJ/mol.

In the other interaction, one configuration minima was obtained upon optimization, CaAPE3. In the stable structure, the calcium atom acts as a bridge between nitrogen atoms of amine and piperazine moieties. In the other stable conformation, CaAPE4, the piperazine ring has a boat structure and calcium interacts with three nitrogen atoms. The stabilization energies of these interactions are -1487.2987 and -1487.0700 kJ/mol, respectively.

In the other optimized interactions, two minima denoted as CaAPE5 and CaAPE6 were predicted at DFT level. In the most stable configuration, CaAPE6, the four nitrogen atoms trap calcium atom in the hole in which the interaction energy is –1493.9667 kJ/mol. In the CaAPE5 configuration, one piperazine ring has a boat structure and the other piperazine ring has a slight interaction toward calcium. The stabilization energy of this confirmation (-1490.8732 kJ/mol) is about 3.0935 kJ/mol which is less than the one calculated for CaAPE6. Finally, in the CaAPE7 configuration, the APE diamine acts as a chelate ligand. The interaction energy of this conformation is less than the other one (-1489.6220kJ/mol) which is slightly smaller than the other structures which were denoted to infrastructure pressure.

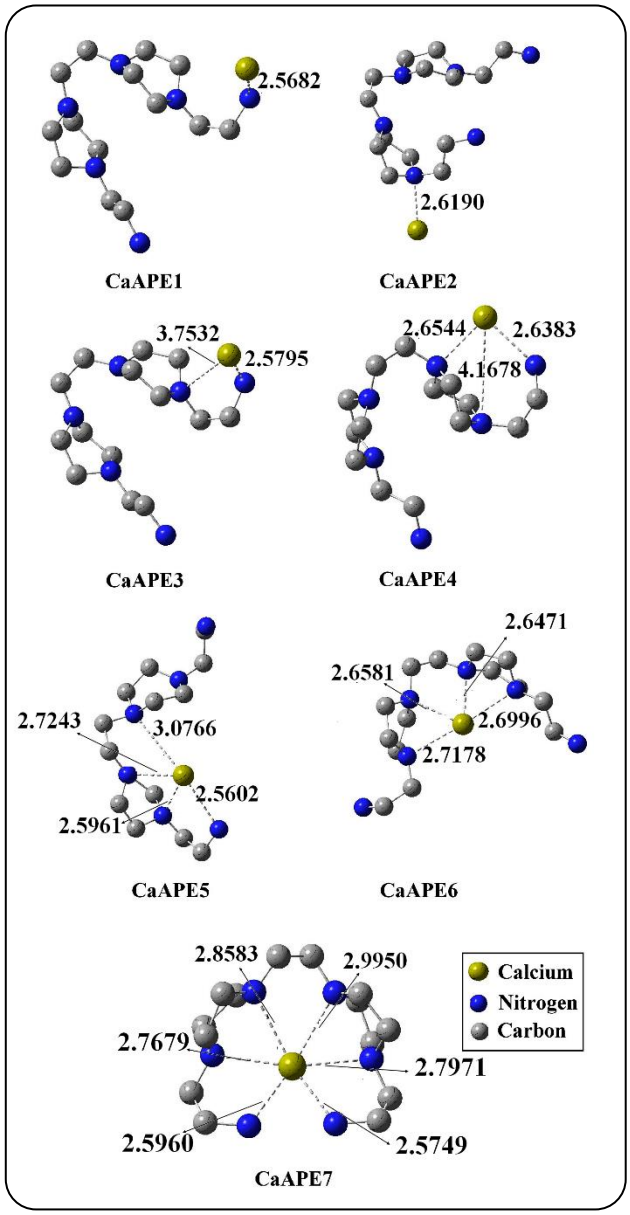

Fig. 2: Molecular graph of calcium and APE at the B3LYP/6-311++G(p,d) level and interatomic distances (A°) of the intermolecular interactions.

Neuroprotective effects

Fluorescent staining was used to determine apoptotic cell death based on morphological changes (Fig. 3). In freshly prepared slices (0 hour) motor neurons showed a large cell body, large nucleus, and the expected distribution of nuclear material, and no apoptotic signs could be observed within the motor neurons (Fig. 3a). After 24 hours, many motor neurons displayed morphological futures of apoptosis such as cell shrinkage as well as nuclear and chromatin condensation (Fig. 3b). The application

Table 1: Percentage of motor neuron viability and diameter of motor neuron nucleus at 0 hour and 24 hours in the absence (control) or presence of APE (50 µM) and LPE (25, 50, 100 and 200 µM)

	Oh	24h (control)	APE	LPE
Motor neuron viability (%)	99.93±0.10[a]	46.17±3.19[a]	90.17±1.60[a]	47.83±2.32[a]
Diameter of motor neuron nucleus (µ	10.75±0.60[a]	6.74±0.19[a]	8.82±0.16[a]	7.03±0.51[a]

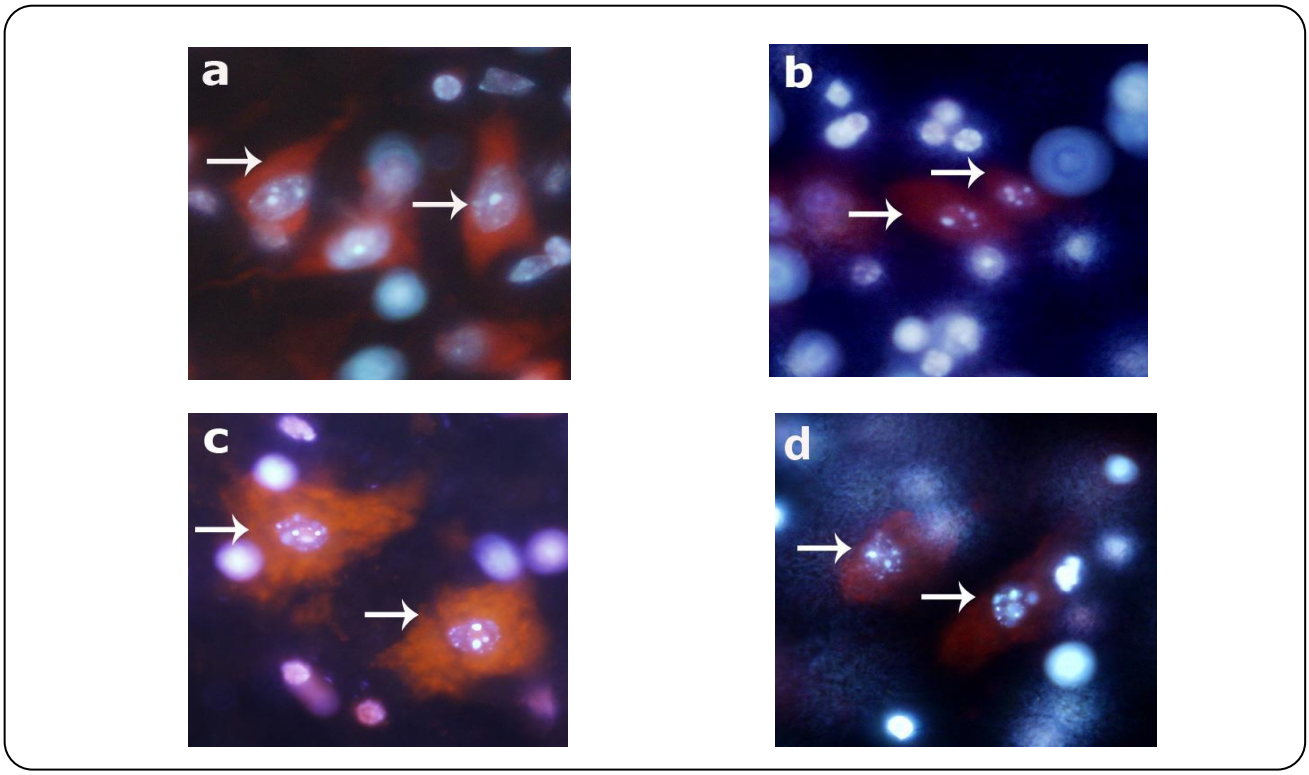

Fig. 3: The inhibition of apoptosis in motor neurons. Motor neurons were stained with a combination of propidium iodide (red) and Hoechst (blue). a: Motor neurons with no apoptotic sign at 0 hour. b: Motor neurons from slices cultured for 24 hours (control) showed nuclear and chromatin condensation. APE, 50 µM, (c) inhibited nuclear apoptotic changes after 24 hours compared to the control. However, LPE (d) with the concentration of 25, 50, 100 and 200 µM had no effect. Arrows show motor neurons. Magnification: 400X.

of APE (50 µM), as an effective concentration, considerably prevented the appearance of nuclear apoptotic changes in the motor neurons after 24 hours (Fig. 3c and Table 1) compared to the control (Fig. 3b). Furthermore, APE significantly ($p<0.001$) increased the percentage of motor neuron viability in the ventral horns after 24 hours as compared with the control (Table 1). However, LPE (25-50-100-200 µM) had an effect neither on apoptosis inhibition nor on the viability of the motor neurons (Fig. 3d and Table 1).

Piperazine-compounds have demonstrated to exert a neuroprotective role [47]. How and by which mechanism APE could effectively prevent apoptosis in the motor neurons remained to be investigated. One possibility might be related to its amine groups. Although polyamines have shown to induce apoptosis in breast cancer cells [48], more evidence points to the involvement of polyamines in cell growth, cell viability, and the inhibition of apoptosis [49].

Excessive intracellular calcium concentration is a major contributor to neuronal death in spinal cord injuries and neurodegenerative disorders [50]. Under pathological conditions, an elevated cytosolic Ca^{2+} concentration can activate Ca^{2+}-dependent proteases, calpain, and/or endonucleases [42], leading to apoptosis. Increased calpain activity has also been reported in the motor neurons of adult mouse spinal cord slices in culture [42].

Studies have also shown that EGTA as a potent calcium chelator could inhibit apoptosis in the motor neurons of the spinal cord [42]. We, therefore, hypothesized that apoptosis may induce in the motor neurons of cultured spinal cord slices by an increase in intracellular Ca^{2+} concentration. If our hypothesis was true, the application of calcium chelators could prevent the occurrence of apoptosis in the motor neurons. In this study, we showed that the application of APE not only inhibited apoptosis in the motor neurons but also significantly increased viability in these neurons. Since diamine compound display Ca^{2+} chelating property [42, 51], it is therefore reasonable to assume that APE with its property in chelating Ca^{2+} acts as an anti-apoptotic agent which in turn exerts its neuroprotective effect on apoptosis of the motor neurons.

In this study, we showed that LPE could not prevent the apoptosis of the motor neurons. It may be due to inter and/or intramolecular hydrogen bonds between azomethine and phenol moieties [52] and therefore the compound is not able to coordinate with the cations as effective as APE. This weakness might explain why LPE with the used concentration had no effects on the inhibition of apoptosis in the motor neurons.

CONCLUSIONS

Synthesis, FT-IR, ^{1}H and $^{13}C\{^{1}H\}$NMR and UV–Vis data of new piperazine-based compounds, APE and LPE, are reported. The prepared compounds were evaluated for their preventive effect on apoptotic motor neurons in adult mouse spinal cord slices. The application of LPE not only inhibited apoptosis in the motor neurons but also significantly increased viability in these neurons; while diamine compound, APE, display Ca^{2+} interaction property. This LPE behavior may be due to inter and/or intramolecular hydrogen bonds between azomethine and phenol moieties which are not able to coordinate to calcium ions.

Also, the Optimized geometries of prepared compounds were also obtained. The geometrical structures of APE and Calcium atoms in the gas phase have been investigated and the interaction structures characterized contain N…Ca attractive interaction with stabilization energies in the range -1481.0711– -1493.9667 kJ/mol.

Received : Aug. 27, 2019 ; Accepted :Dec. 2, 2019

REFERENCES

[1] Mao Z., Zheng X., Qi Y., Zhang M., Huang Y., Wan C., Rao G., Synthesis and Biological Evaluation of Novel Hybrid Compounds Between Chalcone and Piperazine as Potential Antitumor Agents, *J. RSC Adv.*, **6**: 7723-7727 (2016).

[2] Kazemi S., Ghaemi A., Tahvildari K., Chemical Absorption of Carbon Dioxide Into Aqueous Piperazine Solutions Using a Stirred Reactor, *Iran. J. Chem. Chem. Eng. (IJCCE)*, **39(4)**: 253-267 (2020).

[3] Mao A.W., Zheng X., Lin Y.P., Hu C.Y., Wang X.L., Wan C.P., Rao G.X., Design, Synthesis and Anticancer Activity of Novel Hybrid Compounds Between Benzofuran and N-Aryl Piperazine: Biological Activity and Synthesis, *Bioorg. Med. Chem. Lett.*, **26**: 3421-3424 (2016).

[4] Mazari S.A., Ali B.S., Jan B.M., Saeed I.M., Degradation Study of Piperazine, Its Blends and Structural Analogs for CO_2 Capture*:* A Review, *Int. J. greenth Gas Con.*, **31**: 214-228 (2014).

[5] Lee C.C., Hsu S.C., Lai L.L., Lu K.L., Chair-Boat Form Transformation of PiperazineContaining Ligand Toward the Preparation of Dirhenium Metallacycles, *Inorg. Chem.*, **48**: 6329-6331 (2009).

[6] Nagy P.I., Maheshwari A., Kim Y.-W., Messer W.S., Theoretical and Experimental Studies of the Isomeric Protonation In Solution for a Prototype Aliphatic Ring Containing Two Nitrogens, *J. Phys. Chem. B.*, **114**: 349-360 (2010).

[7] Samie N., Muniandy S., Kanthimathi M.S., Haerian B.S., Mechanism of action of Novel Piperazine Containing a Toxicant Against Human Liver Cancer Cells, *Peer J.*, **4**: e1588 (2016).

[8] Pu S.Z., Sun Q., Fan C.B., Wang R.J., Liu G., Recent Advances in Diarylethene-Based Multi-Responsive Molecular Switches, *J. Mater. Chem. C.*, **4**: 3075-3093 (2016).

[9] Chen Y., Wang X.C, Xu Y.C., Xu H.L., Yuan H., Tong J.T., Xiao D.R., Syntheses, Structures and Magnetism of four Ni(II)/Co(II) Interpenetrating Coordination Polymers Based on 1,4-bis(4-(imidazole-1-yl)benzyl)piperazine, *Inorganica Chimica Acta*, **451**: 1-7 (2016).

[10] Moisescu-Goia C., Muresan-Pop M., Simon V., New Solid State Forms of Antineoplastic 5-Fluorouracil with Anthelmintic Piperazine, *J. Mol. Struct.*, **1150**: 37-43 (2017).

[11] Bogdanov E.V., Vazykhova A.M., Khasiyatullina N.R., Krivolapov D.B., Dobrynin A.B., Voloshina A.D., Mironov V.F., New N-Mannich Bases Obtained From Isatin and Piperazine Derivatives: the Synthesis and Evaluation of Antimicrobial Activity, *Chem. Heterocycl. Compd.*, **52(1)**: 25-30 (2016).

[12] Harshad P.L., Dhruvin R.S., KishorH.C., The Novel Derivatives of 3-(iminomethyl)-2H-chromen-2-one with Thiourea and Piperazine Structural Motive: Rationale, Synthesis, Antimicrobial and Anti-TB Evaluation, *Lett. Drug des. Discov.*, **12**: 324-341 (2018).

[13] Sadashiva C.T., Narendra Sharath Chandra J.N., Ponnappa K.C., Veerabasappa Gowda T., Rangappa K.S., Synthesis and Efficacy of 1-[Bis(4-Fluorophenyl)-Methyl]Piperazine Derivatives for Acetylcholinesterase Inhibition, as a Stimulant of Central Cholinergic Neurotransmission in Alzheimer's Disease, *Bioorg Med Chem Lett*, **16**: 3932-6 (2006).

[14] Nozawa D., Okubo T., Ishii T., Takamori K., Chaki S., Okuyama S., Nakazato A., Novel Piperazines: Potent Melanocortin-4 Receptor Antagonists with Anxiolytic-Like Activity, *Bioorg Med Chem*, **15**: 2375-85 (2007).

[15] Nakhaei A., Davoodnia A., Yadegarian S., An Efficient Green Approach for the Synthesis of Fluoroquinolones Using Nano Zirconia Sulfuric Acid as Highly Efficient Recyclable Catalyst in two Forms of Water, *Iran. J. Chem. Chem. Eng*, **37(3)**: 33-42 (2018).

[16] Staack R.F., Paul L.D., Springer D., Kraemer T., Maurer H.H., Cytochrome P450 Dependent Metabolism of the New Designer Drug 1-(3-Trifluoromethylphenyl)Piperazine (TFMPP). *In Vivo* Studies in Wistar and Dark Agouti Rats as Well as in Vitro Studies in Human Liver Microsomes, *Biochem Pharmacol*, **67**: 235-44 (2004).

[17] Chander S., Ashok P., Reguera R.M., Perez-Pertejo M.Y., Carbajo-Andres R., Balana-Fouce R., Gowri K.V., Sekhar C., Sankaranarayanan M., Synthesis and Activity of Benzopiperidine, Benzopyridine and Phenyl Piperazine Based Compounds Against Leishmania Infantum, *Exp. Parasitol.*, **189**: 49-60 (2018).

[18] Guo J., Tao H., Alasadi A., Huang Q., Jin S., Niclosamide Piperazine Prevents High-Fat Diet-Induced Obesity and Diabetic Symptoms in Mice, *Eat Weight Disord-ST.*, **24(1)**: 91-96 (2019).

[19] Cardosi M., Kirkwood S., Electron transfer agent, *US Patent App*. 15/569,901, (2018)

[20] Rajkumar R., Praveen Kumar P., Optical, Mechanical, Dielectric and Thermal Properties of Piperazinium Benzoate single Crystal for Nonlinear Optical Applications, *J. Opt*, **47(1)**: 75–82 (2018).

[21] Saadeh H.A., Khasawneh M.A., Abu-Zeid Y.A., El-Haty E.A., Mubarak M.S., Pechangou Nsangou S., Goyal K., Sehgal R., Marco-Contelles J., Samadi A., Novel 5-Nitroimidazole and 5-Nitrothiazole Piperazine Derivatives and Their Antiparasitic Activity, *ChemistrySelect*, **2(20)**: 5684-5687 (2017).

[22] El-Sherif A.A., Shehata M. R., Shoukry M.M., Mahmoud N., Potentiometric Study of Speciation and Thermodynamics of Complex Formation Equilibria of Diorganotin(IV) Dichloride with 1-(2-Aminoethyl)piperazine, *J Solution Chem.*, **45(3)**: 410–430(2016).

[23] Özbek N., Mamaş S., Erdoğdu T., Alyar S., Kaya K., Karacan N., Synthesis, Characterization, DFT Studies of Piperazine Derivatives And its Ni(II), Cu(II) Complexes as Antimicrobial Agents and Glutathione Reductase Inhibitors, *J. Mol. Struct.*, **1171**: 834-842 (2018).

[24] Bjelogrlić S., Todorović T.R., Cvijetić I., Rodić M.V., Vujčić M., Marković S., AraškovJ., Janović B., Emhemmed F., Muller C.D., Filipović N.R., A Novel Binuclear Hydrazone-Based Cd(II) Complex is a Strong Pro-Apoptotic Inducer with Significant Activity Against 2D and 3D Pancreatic Cancer Stem Cells, *J. Inorg. Biochem*, **190**: 45-66 (2019).

[25] Meena P., Manral A., Saini V., Tiwari M., Protective Effects of a Piperazine Derivative [N-{4-[4-(2-methoxy-phenyl)-piperazin-1-yl]-phenyl} Carbamic acid ethyl ester] Against Aluminium-Induced Neurotoxicity: Insights from in Silico and *in Vivo* Studies, *Neurotox Res*, **27**: 314-27 (2015).

[26] Dolè Kerim M., El Kaïm L., Piperazine as Leaving Group in A3 Adducts: Fast Access to Alkynyl Indoles, *Synlett*, **27(10)**: 1572-1576 (2016).

[27] Wang Y.Y., Bode J.W., Olefin Amine (OLA) Reagents for the Synthesis of Bridged Bicyclic and Spirocyclic Saturated N-Heterocycles by Catalytic Hydrogen Atom Transfer (HAT) Reactions, *J. Am. Chem. Soc.*, **141**: 9739-9745 (2019).

[28] Wang J., Gu Z., Synthesis of 2-(1-Alkoxyvinyl)anilines by Palladium/Norbornene-Catalyzed Amination Followed by Termination with Vinyl Ethers, *Adv. Synth. Catal.*, **358(18)**: 2990-2995 (2016).

[29] Keypour H., Rezaeivala M., Valencia L., Pérez-Lourido P., Synthesis and Crystal Structure of Mn (II) Complexes with Novel Macrocyclic Schiff-Base Ligands Containing Piperazine Moiety, *Polyhedron*, **27:** 3172-3176 (2008).

[30] Khedhiri L., Mi J.X., Rzaigui M., Nasr B., Synthesis, Crystal Structure and Magnetic Properties of 1-(2,5-dimethylphenyl)piperazine-1,4-dium tetrachloridocuprate(II), *J. Chem. Sci.* **128(6)**: 905–911 (2016).

[31] Keypour H., Mahmoudabadi M., Shooshtari A., Bayat M., Karamian R., Asadbegy M., William Gable R., Synthesis, Crystal Structure, Theoretical Studies and Biological Properties of Three Novel Trigonal Prismatic Co(II), Ni(II) and Cu(II) Macroacyclic Schiff Base Complexes Incorporating Piperazine Moiety, *Inorganica Chim. Acta*, **478**: 176-186 (2018).

[32] Sayin S., Soner Engin M., Eymur S., Çay S., Synthesis and Characterization of 1-(2-Furoyl) Piperazine Calix[4]arene for the Preconcentration of Metal Ions, *Anal. Lett.*, **51**: 111-118 (2017).

[33] Almotawa R.M., Aljomaih G., Vargas Trujillo D., N. Nesterov V., Rawashdeh-Omary M.A., New Coordination Polymers of Copper(I) and Silver(I) with Pyrazine and Piperazine: A Step Toward "Green" Chemistry and Optoelectronic Applications, *Inorg. Chem.*, **57(16)**: 9962-9976 (2018).

[34] O'BoyleN.M., Ana G., Kelly P.M., Nathwani S.M., Noorani S., Fayne D., Bright S.A., Twamley B., Zisterer D.M., Meegan M.J., Synthesis and Evaluation of Antiproliferative Microtubule-Destabilising Combretastatin A-4 Piperazine Conjugates, *Org. Biomol. Chem.*, **17**: 6184-6200 (2019).

[35] Kumar M., Gaur N., Sharma B., Singh D.P., Kumar A., Comparative Efficacy of Piperazine, Ivermectin and Levamisole in Spontaneous Toxocariasis in Canines based on Faecal Egg Count and Haemato-Biochemical Changes, *Intas. Polivet.*, **18(1)**: 166-174(2017).

[36] Rodriguez de Barbarin C.O., Bailey N.A, Fenton D.A., He Q.Y., Zinc(II) Complexes Derived from Potentially Hexadentate (N4O2)Acyclic Ligands Containing Pyridinyl and Phenolic Groups, *J. Chem. Soc., Dalton Trans.*, 161-166 (1997).

[37] Lachmann D., Studte C., Männel B., Hübner H., Gmeiner P., König B., Photochromic Dopamine Receptor Ligands Based on Dithienylethenes and Fulgides, *Chem. Eur J.*, **23(54)**: 13423-13434 (2017).

[38] Becker I., Preparation of Derivatives of 1-(2-pyrimidinyl)piperazine as Potential Antianxiety, Antidepressant, And Antipsychotic Agents, *J. Heterocyclic Chem*, **45**: 1005-22 (2008).

[39] Choo H.Y., Chung B.J., Chung S.H., Synthesis of Piperazine Derivatives and Evaluation of Their Antihistamine and Antibradykinin Effects, *Bioorg Med. Chem. Lett*, 9: 2727-30 (1999).

[40] Meena P., Manral A., Saini V., Tiwari M., Protective Effects of a Piperazine Derivative [N-{4-[4-(2-methoxy-phenyl)-piperazin-1-yl]-phenyl} carbamic Acid Ethyl Ester] Against Aluminium-Induced Neurotoxicity: Insights from in Silico and *In Vivo* Studies, *Neurotox Res*, **27**: 314-27 (2015).

[41] Frisch M.J., Trucks G.W., Schlegel H.B., Scuseria G.E., Robb M.A., Cheeseman J.R., Montgomery J.A., Vreven T., Kudin K.N., Burant J.C., Millam J.M., Iyengar S.S., Tomasi J., Barone V., Mennucci B., Cossi M., Scalmani G., Rega N., Petersson G.A., Nakatsuji H., Hada M., Ehara M., Toyota K., Fukuda R., Hasegawa J., Ishida M., Nakajima T., Honda Y., Kitao O., Nakai H., Klene M., Li X., Knox J.E., Hratchian H.P., Cross J.B., Adamo C., Jaramillo J., Gomperts R., Stratmann R.E., Yazyev O., Austin A.J., Cammi R., Pomelli C., Ochterski J.W., Ayala P.Y., Morokuma K., Voth G.A., Salvador P., Dannenberg J.J., Zakrzewski V.G., Dapprich S., Daniels A.D., Strain M.C., Farkas O., Malick D.K., Rabuck A.D., Raghavachari K., Foresman J.B., Ortiz J.V., Cui Q., Baboul A.G., Clifford S., Cioslowski J., Stefanov B.B., Liu G., Liashenko A., Piskorz P., Komaromi I., Martin R.L., Fox D.J., Keith T., Al-Laham M.A., Peng C.Y., Nanayakkara A., Challacombe M., Gill P.M.W., Johnson B., Chen W., Wong M.W., Gonzalez C., Pople J.A., Gaussian 03, Gaussian, Inc., *Pittsburgh PA*, (2003).

[42] Momeni H.R., Kanje M., Calpain Inhibitors Delay Injury-Induced Apoptosis in Adult Mouse Spinal Cord Motor Neurons, *Neuroreport*, **17**: 761-5 (2006).

[43] Keypour H., Rezaeivala M., Valencia L., Pérez-Lourido P., Synthesis and Crystal Structure of Mn (II) Complexes with Novel Macrocyclic Schiff-Base Ligands Containing Piperazine Moiety, *Polyhedron*, **27**: 3172-3176 (2008).

[44] Khanmohammadi H., Abnosi M.H., Hosseinzadeh A., Erfantalab M., Synthesis, Biological and Computational Study of New Schiff Base Hydrazones Bearing 3-(4-pyridine)-5-mercapto-1,2,4-triazole Moiety, *Spectrochim Acta A Mol Biomol Spectrosc*, **71**: 1474-80 (2008).

[45] Krishnakumar V., Xavier R.J., FT Raman and FT-IR Spectral Studies of 3-mercapto-1,2,4-triazole, *Spectrochim. Acta A. Mol. Biomol. Spectrosc.*, **60**: 709-14 (2004).

[46] El-Behery M., El-Twigry H., Synthesis, Magnetic, Spectral, and Antimicrobial Studies of Cu(II), Ni(II) Co(II), Fe(III), and UO2(II) Complexes of a new Schiff Base Hydrazone Derived from 7-chloro-4-Hydrazinoquinoline, *Spectrochim. Acta A. Mol. Biomol. Spectrosc.*, **66**: 28-36 (2007).

[47] Sallem W., Serradji N., Dereuddre-Bosquet N., Dive G., Clayette P., Heymans F., Structure-Activity Relationships in Platelet-Activating Factor. Part 14: Synthesis and Biological Evaluation of Piperazine Derivatives with Dual Anti-PAF and Anti-HIV-1 activity, *Bioorg. Med. Chem.*, **14**: 7999-8013 (2006).

[48] Holst C.M., Frydman B., Marton L.J., Oredsson S.M., Differential Polyamine Analogue Effects in Four Human Breast Cancer Cell Lines, *Toxicology*, **223**: 71-81 (2006).

[49] Harada J., Sugimoto M., Polyamines Prevent Apoptotic Cell Death in Cultured Cerebellar Granule Neurons, *Brain. Res.*, **753**: 251-9 (1997).

[50] Ray S.K., Hogan E.L., Banik N.L., Calpain in the Pathophysiology of Spinal Cord Injury: Neuroprotection with Calpain Inhibitors, *Brain. Res. Rev.*, **42**: 169-185 (2003).

[51] Kajitani N., Kobuchi H., Fujita H., Yano H., Fujiwara T., Yasuda T., Utsumi K., Mechanism of A23187-Induced Apoptosis In HL-60 Cells: Dependency on Mitochondrial Permeability Transition but not on NADPH Oxidase, *Biosci. Biotechnol. Biochem.*, **71**: 2701-11 (2007).

[52] Salavati-Niasari M., Bazarganipour M., Effect of Single-Wall Carbon Nanotubes on Direct Epoxidation of Cyclohexene Catalyzed by New Derivatives of Cis-Dioxomolybdenum(VI) Complexes with Bis-Bidentate Schiff-Base Containing Aromatic Nitrogen-Nitrogen Linkers, *J. Mol. Catal. A Chem.*, **278**: 173-180 (2007).